Proximity effect in ferromagnet–superconductor hybrid structures: role of the pairing symmetry

N Stefanakis and R Mélin

Centre de Recherches sur les Très Basses Températures, Centre National de la Recherche
Scientifique, 25 Avenue des Martyrs, BP 166, 38042 Grenoble cédex 9, France

Abstract
The spatial variations of the pair amplitude and the local density of states in
d- or s-wave superconductor–ferromagnet (SF) hybrid structures are calculated
self consistently using the Bogoliubov–de Gennes formalism within the two-
dimensional extended Hubbard model. We describe the proximity effect
in SF bilayers, ferromagnet–superconductor–ferromagnet (FSF) trilayers and
interfaces between a superconductor and a ferromagnetic domain wall. We
investigate in detail the role played by the pairing symmetry, the exchange
field, interfacial scattering and crossed Andreev reflection.

(Some figures in this article are in colour only in the electronic version)

1. Introduction

The determination of the physics associated to d-wave symmetry has become one of the
main aspects in research on high temperature superconductors [1–5]. Tunnelling conductance
experiments report the existence of a zero-bias conduction peak (ZBCP) [6–11]. The origin
of the experimental ZBCP is explained in the context of zero-energy states (ZES) formed
near the [110] surfaces of d-wave superconductors [4, 12, 13]. These ZES do not appear for
s-wave superconductors or near the [100] surface of d-wave superconductors and are one of
the features that characterize d-wave superconductors.

In junctions made of s- or d-wave superconductors connected to normal metals
or ferromagnets, superconducting correlations penetrate in the normal metal or in the
ferromagnetic region, which is called the proximity effect. Landauer formalism or
quasiclassical models have been used to calculate the tunnelling conductance at interfaces
between superconductors and ferromagnetic metals [14–17]. One of the remarkable effects
is the suppression of the tunnelling conductance by spin polarization in the ferromagnet [18].
This effect is related to the fact that Andreev reflection in a multichannel ferromagnet–
superconductor (FS) point contact takes place only in the channels having both a spin-up
and a spin-down Fermi surface. In the studies in [14–17] a simple step function variation for
the order parameter is assumed, and the proximity effect is thus ignored.

For s-wave pairing, the proximity effect has been studied in the dirty limit where the electron mean free path is shorter than the coherence length, by solving the Usadel equations [19, 20]. It has been demonstrated that in a ferromagnetic metal near the boundary with a superconductor the local density of states (LDOS) at energies close to the Fermi energy E_F has a damped-oscillatory behaviour similar to the decay of the Cooper's pair density. This effect has been observed experimentally [21]. Moreover transport in superconductor–ferromagnet–superconductor (SFS) trilayers has been investigated experimentally [22]. For cuprate superconductivity, spin polarized transport experiments suggest strong effects due to spin polarization under the form of a suppression of the critical current [23, 24].

Lattice models have been used to study LDOS for rough surfaces of d-wave superconductors [25], interface properties of s- and d-wave superconductors [26], broken time reversal symmetry pairing state near a surface of a d-wave superconductor [27] and disorder near the corner of d-wave superconductors [28]. Moreover extensive calculations based on the extended Hubbard model have been performed in order to study the spontaneous spin polarized currents in s-wave SF heterostructures [29, 30], and also the proximity effect and relevant length scales in the same structures [31]. As concerning d-wave superconductors, the extended Hubbard model has already been used to study the proximity effect and quasiparticle transport in ferromagnet-d-wave–superconductor junctions [32]. It was found that the proximity-induced d-wave pair amplitude oscillates in the ferromagnetic region as in the case of s-wave pairing. The tunnelling conductance was also discussed in the framework of a scattering approach [32].

In this paper our goal is to explore several new aspects related to the proximity effect in superconductor–ferromagnet (SF) bilayers, ferromagnet–superconductor–ferromagnet (FSF) trilayers and interfaces between a superconductor and a ferromagnetic domain wall (DW). The spatial variation of the pair amplitude and the LDOS are studied as a function of several relevant parameters: the distance from the surface, the exchange field, the barrier strength and the symmetry of the pair potential. The method is based on exact diagonalizations of the Bogoliubov–de Gennes (BdG) equations associated to the mean field solution of an extended Hubbard model. Our predictions from the simulations of this model are of interest in view of future STM spectroscopy experiments on hybrid structures.

The pair amplitude oscillates in the ferromagnetic region both for s- and d-waves, and the period of oscillations decreases with increasing exchange field. The LDOS in the superconductor shows large residual values within the gap due to the proximity effect, which are increased by the increase of the exchange field. In the ferromagnet the proximity effect appears as a peak in the LDOS for s-wave and a mini-gap for d-wave. For both cases the overall LDOS in the ferromagnet is suppressed with the exchange field.

For the d-wave SF bilayer, ZES exist only if there exists a finite barrier potential. This is because ZES are due to back-scattering at the interface in the presence of a sign change in the order parameter. The presence of a strong barrier decouples the superconductor from the ferromagnet and therefore suppresses the proximity effect. For a S/DW interface the zero-energy peak (ZEP) in the LDOS appears also in the d-wave case due to the constructive interference of the ZES that originate from each domain. For FSF trilayers the pair amplitude is larger in the antiferromagnetic alignment of the magnetizations of the ferromagnetic electrodes, both in the s- and d-wave cases. This can be contrasted with recent discussions based on different models [20, 33]. We provide here simple physical arguments to explain our numerical results in terms of (a) local and non-local Andreev reflections and (b) pair breaking effects.

The paper is organized as follows. In section 2 we develop the model and discuss the formalism. In section 3 we discuss the effect of the exchange field. In section 4 we discuss the effect of the strength of the barrier. In section 5 we discuss the effect of an inhomogeneous

exchange field. In section 6 we present the ferromagnet–superconductor–ferromagnet trilayer. Finally a summary and discussions are presented in the last section.

2. BdG equations, for the superconductor–ferromagnet junction within the Hubbard model

The Hamiltonian of the extended Hubbard model on a two-dimensional square lattice takes the form

$$
H = -t \sum_{\langle i,j \rangle \sigma} c_{i\sigma}^{\dagger} c_{j\sigma} + \mu \sum_{i\sigma} n_{i\sigma} + \sum_{i\sigma} \mu_i^I n_{i\sigma} + \sum_{i\sigma} h_{i\sigma} n_{i\sigma}
$$
$$
+ V_0 \sum_i n_{i\uparrow} n_{i\downarrow} + \frac{V_1}{2} \sum_{\langle ij \rangle \sigma \sigma'} n_{i\sigma} n_{j\sigma'}, \tag{1}
$$

where i, j are site indices and the angle brackets indicate that the hopping is only to nearest neighbours, $n_{i\sigma} = c_{i\sigma}^{\dagger} c_{i\sigma}$ is the electron number operator at site i, μ is the chemical potential which we set to zero, $h_{i\sigma} = -h_0 \sigma_z$ is the exchange field in the ferromagnetic region and V_0, V_1 are the on-site and nearest-neighbour interaction strengths. Negative values of V_0 and V_1 mean attractive interaction and positive values mean repulsive interaction. When $V_1 < 0$ the pairing interaction gives rise to d-wave superconductivity in a restricted parameter range [34]. In the following we set $V_0 = -2.5t$ and $V_1 = 0$ for the description of the s-wave superconductor, while $V_1 = -2.5t$ and $V_0 = 0$ for the description of the d-wave superconductor. To simulate the effect of depletion of the carrier density at the surface or impurities the site-dependent impurity potential μ_i^I is set to a sufficiently large value at the surface sites. This prohibits electron tunnelling over these sites. Within the mean field approximation equation (1) reduces to the BdG equations [35]:

$$
\begin{pmatrix} \hat{\xi} & \hat{\Delta} \\ \hat{\Delta}^* & -\hat{\xi} \end{pmatrix} \begin{pmatrix} u_{n\uparrow}(r_i) \\ v_{n\downarrow}(r_i) \end{pmatrix} = \epsilon_{n\gamma_1} \begin{pmatrix} u_{n\uparrow}(r_i) \\ v_{n\downarrow}(r_i) \end{pmatrix}, \tag{2}
$$

$$
\begin{pmatrix} \hat{\xi} & \hat{\Delta} \\ \hat{\Delta}^* & -\hat{\xi} \end{pmatrix} \begin{pmatrix} u_{n\downarrow}(r_i) \\ v_{n\uparrow}(r_i) \end{pmatrix} = \epsilon_{n\gamma_2} \begin{pmatrix} u_{n\downarrow}(r_i) \\ v_{n\uparrow}(r_i) \end{pmatrix} \tag{3}
$$

such that

$$
\hat{\xi} u_{n\sigma}(r_i) = -t \sum_{\hat{\delta}} u_{n\sigma}(r_i + \hat{\delta}) + (\mu^I(r_i) + \mu) u_{n\sigma}(r_i) + h_i \sigma_z u_{n\sigma}(r_i), \tag{4}
$$

$$
\hat{\Delta} u_{n\sigma}(r_i) = \Delta_0(r_i) u_{n\sigma}(r_i) + \sum_{\hat{\delta}} \Delta_{\delta}(r_i) u_{n\sigma}(r_i + \hat{\delta}), \tag{5}
$$

where the gap functions are defined by

$$
\Delta_0(r_i) \equiv V_0 \langle c_\uparrow(r_i) c_\downarrow(r_i) \rangle, \tag{6}
$$
$$
\Delta_{\delta}(r_i) \equiv V_1 \langle c_\uparrow(r_i + \hat{\delta}) c_\downarrow(r_i) \rangle \tag{7}
$$

and where $\hat{\delta} = \hat{x}, -\hat{x}, \hat{y}, -\hat{y}$. Equations (2) and (3) are subject to the self consistency requirements

$$
\Delta_0(r_i) = \frac{V_0(r_i)}{2} F_0(r_i) = \frac{V_0(r_i)}{2} \sum_n \left(u_{n\uparrow}(r_i) v_{n\downarrow}^*(r_i) \tanh\left(\frac{\beta \epsilon_{n\gamma_1}}{2} \right) \right.
$$
$$
\left. + u_{n\downarrow}(r_i) v_{n\uparrow}^*(r_i) \tanh\left(\frac{\beta \epsilon_{n\gamma_2}}{2} \right) \right), \tag{8}
$$

$$\Delta_\delta(r_i) = \frac{V_1(r_i + \hat{\delta})}{2} F_\delta(r_i) = \frac{V_1(r_i + \hat{\delta})}{2} \sum_n \left(u_{n\uparrow}(r_i) v_{n\downarrow}^*(r_i + \hat{\delta}) \tanh\left(\frac{\beta\epsilon_{n\gamma_1}}{2}\right) \right.$$
$$\left. + u_{n\downarrow}(r_i + \hat{\delta}) v_{n\uparrow}^*(r_i) \tanh\left(\frac{\beta\epsilon_{n\gamma_2}}{2}\right) \right). \tag{9}$$

We start with approximate initial conditions for the gap functions (8) and (9). After exact diagonalizations of equations (2) and (3) we obtain $u_{n\sigma}(r_i)$ and $v_{n\sigma}(r_i)$ and the eigenenergies $\epsilon_{n\gamma_1}, \epsilon_{n\gamma_2}$. The quasiparticle amplitudes are inserted in equations (8) and (9) and new gap functions $\Delta_0(r_i)$ and $\Delta_\delta(r_i)$ are evaluated. We reinsert these quantities into equations (4) and (5) and we proceed until self-consistency is achieved. We then compute the d-wave and the extended s-wave gap functions given by the expressions [36]

$$\Delta_d(r_i) = \tfrac{1}{4}[\Delta_{\hat{x}}(r_i) + \Delta_{-\hat{x}}(r_i) - \Delta_{\hat{y}}(r_i) - \Delta_{-\hat{y}}(r_i)], \tag{10}$$

$$\Delta_s^{ext}(r_i) = \tfrac{1}{4}[\Delta_{\hat{x}}(r_i) + \Delta_{-\hat{x}}(r_i) + \Delta_{\hat{y}}(r_i) + \Delta_{-\hat{y}}(r_i)]. \tag{11}$$

The pair amplitude for the s-wave case is $F_0(r_i)$. The pair amplitude for the d-wave case is given by the expression

$$F_d(r_i) = \tfrac{1}{4}[F_{\hat{x}}(r_i) + F_{-\hat{x}}(r_i) - F_{\hat{y}}(r_i) - F_{-\hat{y}}(r_i)]. \tag{12}$$

The LDOS at the ith site is given by

$$\rho_i(E) = -\sum_{n\sigma}[|u_{n\sigma}(r_i)|^2 f'(E - \epsilon_n) + |v_{n\sigma}(r_i)|^2 f'(E + \epsilon_n)], \tag{13}$$

where f' is the derivative of the Fermi function

$$f(\epsilon) = \frac{1}{\exp(\epsilon/k_B T) + 1}. \tag{14}$$

3. Effect of the exchange field

We start our investigation of multiterminal hybrid structures by discussing the effect of the exchange field on the pair amplitude and the LDOS in the cases of s- and d-wave symmetry. We consider a two-dimensional system of 30×30 sites and we impose fixed boundary conditions by setting the impurity potential $\mu^I = 100t$ at the surface. The temperature is $k_B T = 0.1t$. The interface is modelled by a line of impurities along the diagonal of the lattice, in the y' direction, where the chemical potential on this line of impurities is set to a value related to the strength of the barrier (see figure 1). The region $x' > 0$, where $V_0 = V_1 = 0$ and h is different from zero, represents the ferromagnet. The region $x' < 0$ is considered as the s- or d-wave superconductor, depending on the presence of nearest-neighbour interactions in the BdG Hamiltonian.

Both in the s- and d-wave cases, the proximity-induced pair amplitude for $h = 0$ decays monotonically in the normal-metal region and oscillates around zero for a finite exchange field in the ferromagnetic region. The period of oscillations decreases with increasing the exchange field, as seen in figure 2.

In the superconducting region the s-wave pair amplitude at the interface is enhanced for $h = 0$ since the interface is not pair breaking. As seen in figure 2(a) the pair amplitude in the superconducting region is modulated by the exchange field and shows $2k_F$ oscillations. In particular the pair amplitude is suppressed by increasing the exchange field since the interface becomes pair breaking. Contrary to the s-wave case the pair amplitude for the d-wave case is suppressed for all values of the exchange field since the interface itself is pair breaking. Also, as seen in figure 2(b) the pair amplitude is not modulated in the superconducting region, which should be contrasted with the s-wave case in figure 2(a).
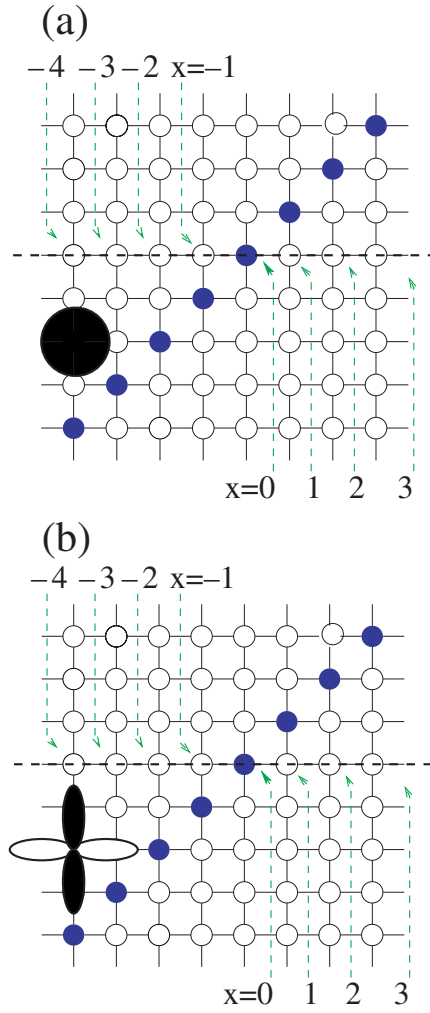
Figure 1. (a) Spatial distribution of impurities in the y' direction, indicated as full circles, corresponding to a s-wave SF interface along the [110] surface. The labelling of the sites along the x direction is also shown. (b) is the same as (a) but for a d-wave. The region $x' > 0$ represents the ferromagnet and the region $x' < 0$ represents the s- or d-wave superconductor.
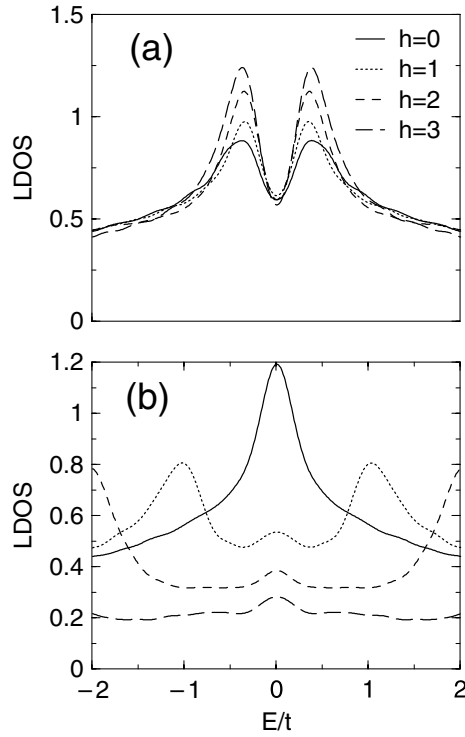
In the s-wave case the LDOS in the ferromagnet decreases with increasing the exchange field, as seen in figure 3(b). For $h = 0$ a single peak exists at $E = 0$. This peak is due to the shape of the LDOS of the two-dimensional lattice model that we use in the simulations. It actually originates from the Van Hove singularity in a nearest-neighbour tight-binding model. There is also an extra contribution to this peak due to the proximity effect. For a finite exchange field two peaks exist symmetrically around zero at $E = \pm h$, since the spin-up and spin-down bands are shifted with respect to the Fermi energy in the presence of the exchange field. These peaks have been observed in STM experiments for the proximity effect of magnetic particles of cobalt included in a niobium layer [37]. The asymmetry observed in the experiment is due to the depletion of the chemical potential in the magnetic region. The long range proximity-induced LDOS in the ferromagnet at the exchange energy has also been found in the diffusive
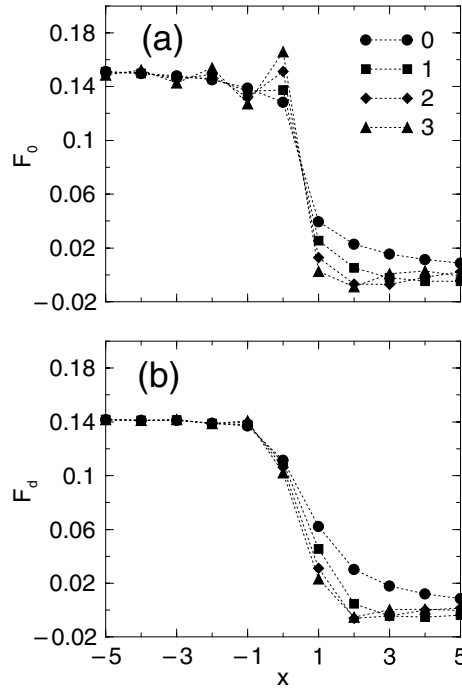
Figure 2. (a) The s-wave superconducting pair amplitude as a function of x for a SF interface for different values of the exchange field $h = 0, 1, 2, 3$ (in units of t). The pair amplitude is calculated along the thick broken line in the direction x shown in figure 1. The chemical potential in the barrier is $\mu^I = 0$. (b) The same as (a) but for d-wave pairing.

limit described by Usadel equations [19]. Also we find that the zero-energy LDOS is enhanced in the ferromagnet (which we call a 'reversal of the gap region'), as opposed to the fact that the zero-energy LDOS is reduced in the superconductor. The reversal of the gapped region in the s-wave case is in agreement with the experiments in [21]. In the superconducting region the LDOS develops a gap (see figure 3(a)). However, due to the proximity effect residual values of the LDOS exist within the gap which correspond to the two peaks in the LDOS in figure 3(a). The residual values of the LDOS depend on the exchange field and have a larger contribution for a larger exchange field as expected. This can be understood from the fact that pair-breaking effects increase with the exchange field in the ferromagnet. As a consequence there is an increase of quasiparticle states within the gap if we increase the exchange field in the ferromagnet which constitutes a qualitative explanation to figure 3(a). We can provide another qualitative explanation in terms of local Andreev reflections in the ferromagnetic electrode which decrease as we increase the exchange field. As a consequence the transfer of Cooper pairs in the superconductor decreases and the LDOS in the superconductor increases. Both arguments apply also in the d-wave case (see figure 4).

The presence of residual values in the LDOS due to the proximity effect is also a property of d-wave SF interfaces as seen in figure 4. The lineshape of the LDOS is V in the case of d-wave symmetry whereas the lineshape was U in the s-wave case. Increasing the exchange field increases the residual values in the gap in the superconductor (see figure 4(a)). We see from figure 4(a) that two energy scales are involved in the LDOS for d-wave symmetry of the order parameter. For instance, in figure 4(a) a local maximum of the LDOS is obtained

Figure 3. The LDOS for the s-wave case as a function of E/t for the site $x = 0$ in the barrier (a) and $x = 1$ in the ferromagnet (b), shown in figure 1, for different values of the exchange field $h = 0, 1, 2, 3$. The chemical potential in the barrier μ^I is zero.

at high energy for $E/t \simeq 1.5$ and a second local maximum is obtained at a lower energy for $E/t \simeq 0.6$. We see in figure 4(a) that the low-energy and high-energy LDOS react differently to the increase of the exchange field. Compared to the s-wave case discussed previously there is an additional pair breaking mechanism in the case of the d-wave which is due to the existence of quasiparticle states within the gap for some orientations. In the case of the [110] interface represented in figure 1 and used in figure 4(a) it is expected that spin polarized electrons from the ferromagnet can penetrate in the superconductor along the direction for which the gap cancels, which is a pair breaking mechanism not present for s-waves.

On the ferromagnetic side of the interface (see figure 4(b)) we do not observe a reversal of the gapped region, unlike the case of a s-wave superconductor in figure 3(b).

The LDOS shows strong modulations with the distance from the interface both for s- and d-wave pairing as seen in figure 5. Increasing the exchange field h increases the residual values of the LDOS in the gap in the superconductor. In both cases the zero-energy density of states oscillates as a function of the distance to the interface as found in experiments [21]. The d-wave gap is more sensitive to the proximity effect of the ferromagnet.

4. Effect of the interfacial scattering potential

In general the increase of the interfacial barrier potential suppresses the proximity effect because the leakage of Cooper pairs from the superconductor to the N or F electrodes is
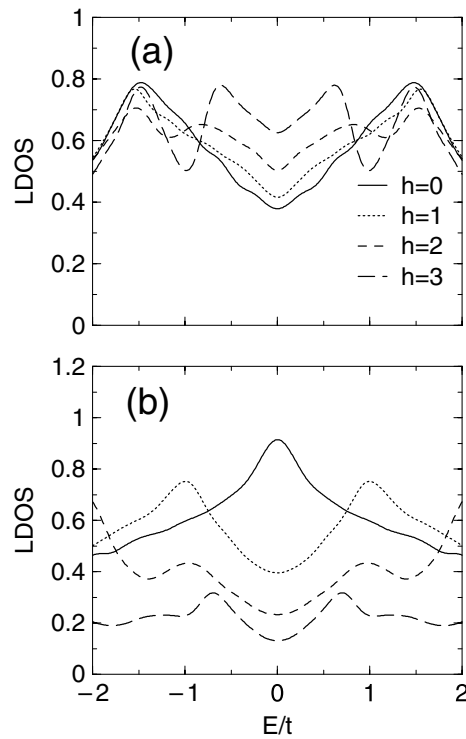
Figure 4. The same as in figure 3 but for d-wave pairing state.

reduced if the tunnel amplitude is reduced. As a consequence, for both s- and d-waves the oscillations of the pair amplitude are reduced on the ferromagnetic side by the increase of the barrier strength, as seen in figure 6. In the s-wave case (see figure 6(a)) the pair amplitude on the superconducting side increases by the increase of the barrier strength since the barrier decouples the superconductor from the ferromagnet and makes the interface less pair breaking. In the d-wave case, on the other hand, the pair amplitude close to the interface is determined by the competition of two effects:

(i) the decoupling of the two layers which makes the interface less pair breaking, and
(ii) the reflection of quasiparticles at the barrier which makes the interface more pair breaking.

As seen in figure 6(b) the latter process dominates over the former and the pair amplitude decreases with the scattering potential on the superconducting side of the interface.

For the s-wave case, the subgap LDOS is suppressed by an increase of the barrier strength and a gap develops on the superconducting side (see figure 7(a)) because the superconductor decouples from the ferromagnet when the barrier strength increases. Moreover the Andreev reflection process is suppressed. On the other hand, it is seen in figure 7(b) that the LDOS on the ferromagnetic site becomes flat (i.e. the peak at zero energy disappears). This proves that the ZEP is due to the proximity effect because the two sides of the interface become decoupled when the strength of the barrier increases. The LDOS in the barrier (not presented) is suppressed since the quasiparticles are not able to tunnel to these sites for very large values of the impurity potential.
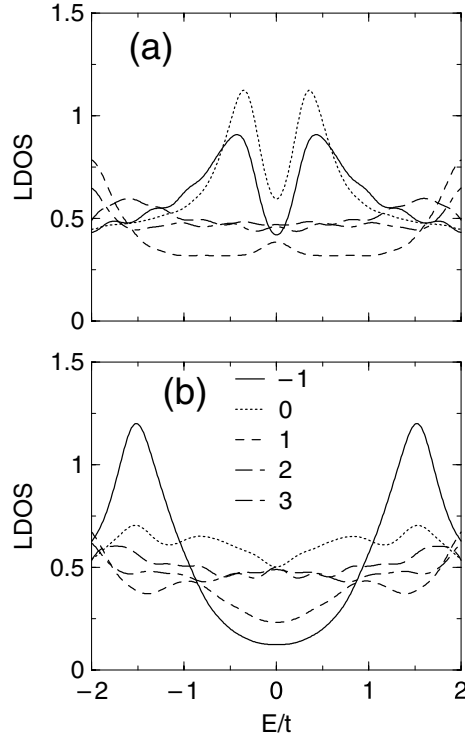
Figure 5. (a) The LDOS as a function of E/t for exchange field $h = 2$ for different values of the distance from the interface $x = -1, 0, 1, 2, 3$. The pairing state is s-wave. (b) The pairing state is d-wave. $x = -1$ is a site in the superconductor. $x = 0$ is a site in the barrier. $x = 1, 2, 3$ are sites in the ferromagnet.

In the d-wave case a ZEP develops and its height increases with increasing barrier strength. Similar behaviour has been obtained for the tunnelling conductance within the quasiclassical theory [4, 13, 38]. Increasing the barrier strength favours the reflection of quasiparticles at the interface and the formation of Andreev bound states due to the sign change of the pair amplitude. This is demonstrated in figure 8(a). The ZES does not exist when the barrier is absent because the quasiparticles are not reflected at the interface. On the ferromagnetic side the mini-gap due to the proximity effect disappears for large barrier strength (see figure 8(b)).

5. Effect of a magnetic domain wall

We want to study the quasiparticle properties in the presence of a magnetic DW. We suppose that the DW is formed in a tricrystal geometry where a superconductor is in contact with a spin-up and a spin-down ferromagnetic domain, as seen in figure 9. We use here a schematic model in which there is no rotation of the magnetization inside the DW. Namely the DW on figure 9 is just a juxtaposition of a spin-up and a spin-down magnetic domain. It is expected that this model is a valid description of the regime where the width of the DW is small compared to the superconducting coherence length. This hypothesis may not be well verified for d-wave superconductors since the superconducting coherence length is very short in high-T_c materials. Nevertheless, even though our model is not fully realistic for d-wave pairing we show that it contains interesting physics that can be a useful guideline for understanding more realistic
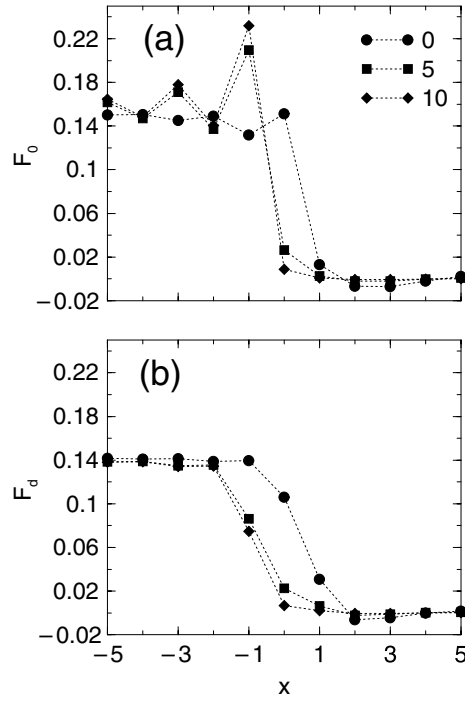
Figure 6. (a) The s-wave superconducting pair amplitude as a function of x, for a SF interface for different values of the interface barrier $\mu^I = 0, 5, 10$ (in units of t). The pair amplitude is calculated along the thick broken line in the direction x shown in figure 1. The exchange field in the ferromagnet is $h = 2$. (b) The same as in (a) but for d-wave pairing.

models in the future. More precisely we want to address the question of the contribution of crossed Andreev reflection to the LDOS and to provide a connection with recent experimental data where a similar geometry is studied with a conventional superconductor [39].

Due to the presence of crossed Andreev reflection we find that, in the s-wave case, the subgap LDOS is smaller than the LDOS at the SF interface with a single spin orientation of the magnetic moment. As we see in 10(a) the subgap LDOS is smaller at the site in front of the DM due to crossed Andreev reflection where a spin-up electron from one domain is reflected as a spin-down hole in the other domain. This process transfers a Cooper pair inside the superconductor and enhances superconductivity. As a consequence the subgap LDOS is reduced. An equivalent explanation can be given in terms of pair breaking close to the DW: the pairs that are formed in front of the DW are more stable because they experience the spin-up and spin-down orientation of the DW. Therefore the effects due to pair breaking are small in DW compared to the SF structure and the subgap LDOS is thus reduced. This behaviour is in agreement with a recent study of multiterminal hybrid structures [33] and with experimental data [39].

In the case of a d-wave order parameter we showed in the previous section that a ZEP is formed at the SF interface only in the presence of a finite barrier strength and d-wave symmetry. The height of the ZEP increases as a function of the barrier strength. In the present section we demonstrate that a magnetic inhomogeneity, e.g. a DW, is also sufficient for the formation of a ZEP in the LDOS in the absence of an impurity potential. This is illustrated in figure 10(b) where the LDOS is plotted as a function of energy along the interface sites for the d-wave case.
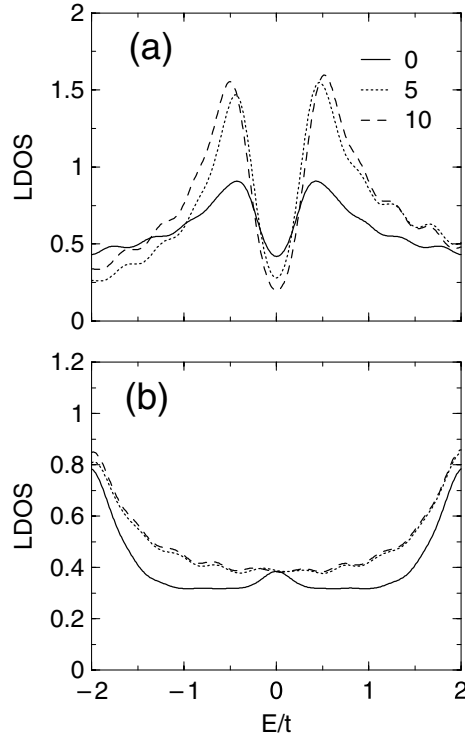
Figure 7. The LDOS for the s-wave case, as a function of E/t for the site $x = -1$ (a) on the superconducting side of the interface and $x = 1$ (b) on the ferromagnetic side of the interface, for different values of the barrier strength $\mu^I = 0, 5, 10$, $h = 2$. The geometry is represented in figure 1.

We see that, far away from the DW, the LDOS does not show a ZEP. However, as we approach the DW a ZEP develops. A first qualitative explanation is crossed Andreev reflection that is affected by the sign change of the order parameter which enhances the zero-energy LDOS. This is qualitatively consistent with [40]. These results can also be well explained in terms of quasiparticle subgap states that originate from the local suppression of the d-wave pairing amplitude very close to the inhomogeneity. In the s-wave case which has been discussed in the previous paragraph, the magnetic inhomogeneity increases superconducting correlations. This is modified in the presence of d-wave superconductivity due to the strong suppression of the order parameter and the formation of quasiparticle states inside the gap.

6. FSF trilayer

Now we describe trilayers consisting of a superconductor inserted in between two ferromagnets. We show that the LDOS and the pair amplitude are controlled by the orientation of magnetizations in the ferromagnets. In particular we find that inside the superconductor the pair amplitude is larger in the antiparallel alignment (see figure 11). This result can be contrasted with recent work [33] in which it was shown from the solution of an analytical model that the superconducting order parameter is larger in the ferromagnetic alignment. The self-consistent approach that we describe here agrees with several analytical solutions that exist in the literature, like the Usadel or Eilenberger equations [19].
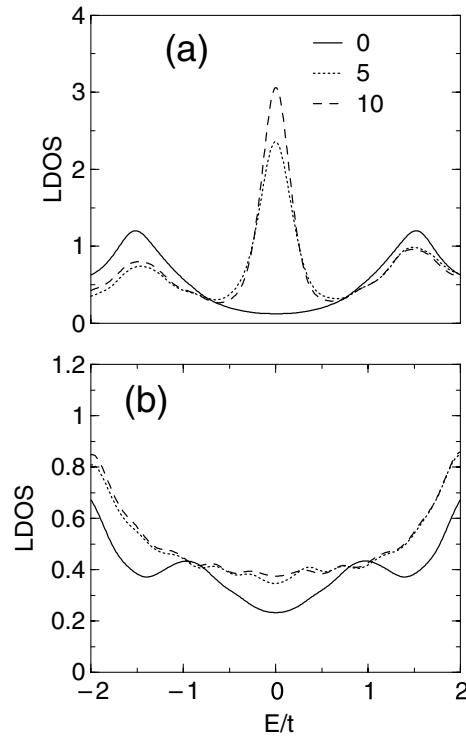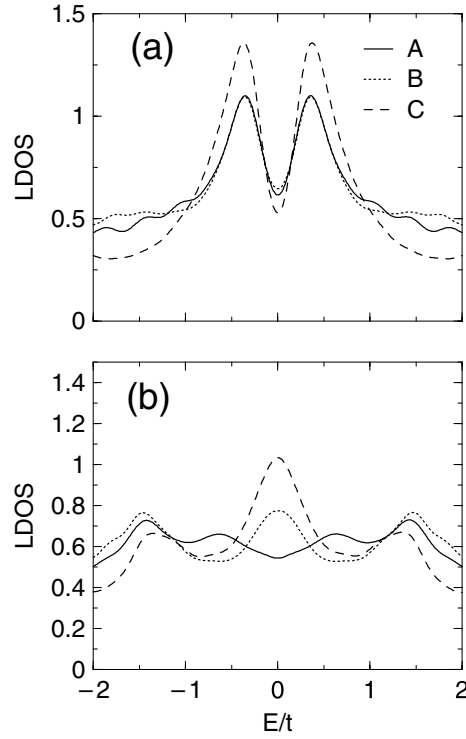
**Figure 8.** The same as in figure 7 but for the d-wave case.
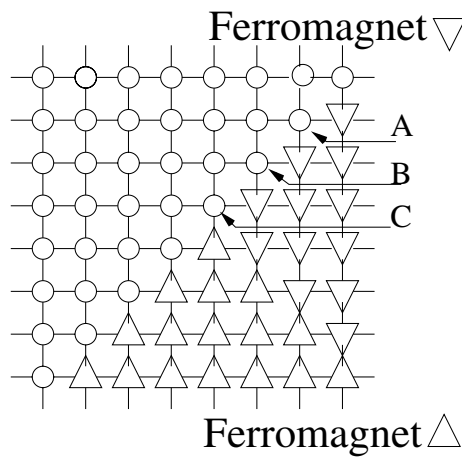
Figure 9. Interface between a s- or d-wave superconductor and a DW between a ferromagnet with spin-up orientation indicated as up-triangles and a ferromagnet with spin-down orientation indicated as down-triangles. The labelling of several sites along the interface is also shown.

For the d-wave case the interface [110] is additionally pair-breaking due to the sign change of the order parameter. As a consequence the effect is much more pronounced than for s-wave, as seen in figure 12. Also, due to the small coherence length of the d-wave superconductor the effect vanishes as soon as the width d of the superconductor is larger than $5a\sqrt{2}$ (where a is
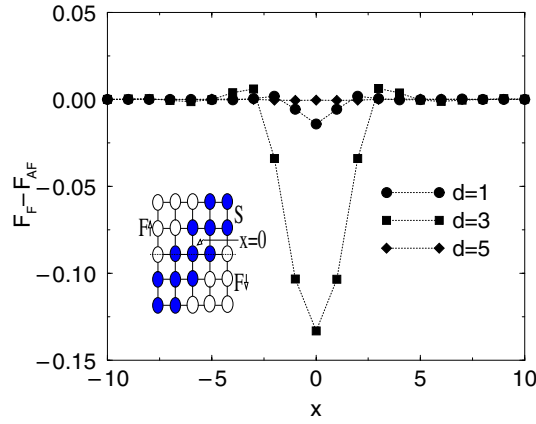
Figure 10. (a) The LDOS for the s-wave case, as a function of E/t for the sites A, B and C shown in the previous figure along the interface. There is no impurity potential at the SF interface. The exchange field is $h = 2$. (b) The same as in (a) but for d-wave. The ZEP is more pronounced at site C for the d-wave case.
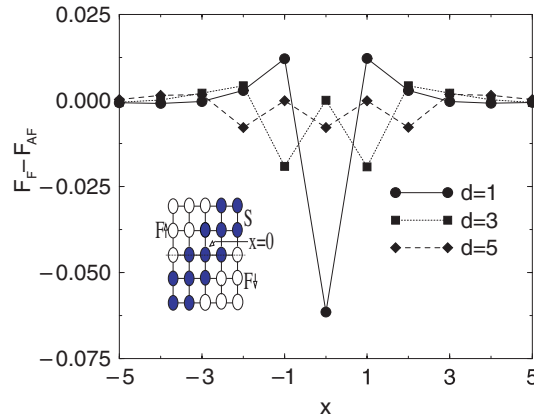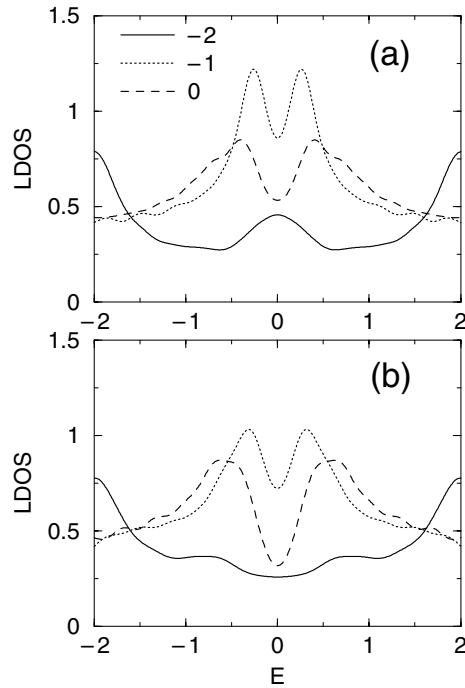

Figure 11. The difference between the pair amplitude in the ferromagnetic and antiferromagnetic alignment of magnetizations for the s-wave case as a function of the distance from the centre of the FSF trilayer (of thickness $d = 3$ in units of $a\sqrt{2}$, where a is the lattice constant) shown in the inset. The exchange field is $h = 2$.

the lattice constant since the interface lies along the [110] direction) in our simulation. Note that for $d = a\sqrt{2}$ we have a very special form of d-wave superconductivity: since the d-wave pairing involves neighbouring sites, normally it is not expected to appear for a one-dimensional
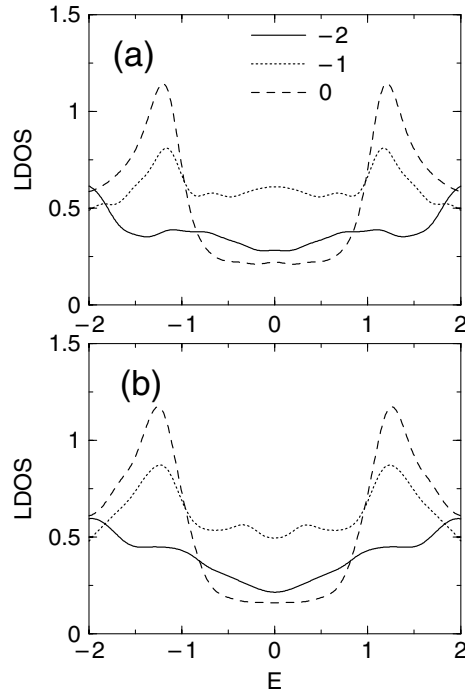
Figure 12. The same as in figure 11 but for the d-wave case.

Figure 13. (a) The LDOS for the s-wave case as a function of E/t for the sites at distance $-2, -1, 0$ from the centre of the trilayer FSF (of thickness $d = 3$ in units of $a\sqrt{2}$, where a is the lattice constant) shown in the previous figure along the interface for the antiferromagnetic alignment of magnetization in the ferromagnetic electrodes. The exchange field is $h = 2$. (b) The same as in (a) but for the ferromagnetic alignment.

superconducting chain. However, in our case the finite d-wave order parameter is due to the proximity effect only.

The LDOS gives information that can be directly compared to tunnelling conductance measurements and STM experiments. For the antiparallel alignment of the spins in the two ferromagnetic electrodes the LDOS shows a gapped structure in the superconductor which is

Figure 14. (a) The LDOS for the d-wave case as a function of E/t for the sites at distance $-2, -1, 0$ from the centre of the trilayer FSF (of thickness $d = 3$ in units of $a\sqrt{2}$, where a is the lattice constant) shown in the previous figure along the interface for the antiferromagnetic alignment of magnetization in the ferromagnetic electrodes. The exchange field is $h = 2$. (b) The same as in (a) but for the ferromagnetic alignment.

enhanced near the boundaries due to the proximity effect, as seen in figure 13(a). In the top sites inside the ferromagnet we see a reversal of the gapped structure as in the proximity effect in bilayers. The same qualitative conclusions hold for the parallel alignment but in this case there is no inverse of the gapped region in the ferromagnet (see figure 13(b)). Similar effects are observed for the d-wave case. Also in this case no reversal of the gapped region is observed in the ferromagnet (see figure 14(b)).

7. Conclusions

We calculated the LDOS and the pair amplitude for several ferromagnet–superconductor hybrid structures self-consistently, within the extended Hubbard model. In SF bilayers we found that the proximity-induced pair amplitude oscillates in the ferromagnetic region. The period of oscillations decreases with increasing exchange field. The pair amplitude is suppressed for the d-wave interface but is enhanced for the s-wave interface. The proximity effect in the LDOS is demonstrated as a peak for s-wave and a mini-gap for d-wave. The LDOS in the superconductor shows large residual values due to the proximity effect which are increased by an increase of the exchange field due to the suppression of Andreev reflection. The barrier decouples the superconductor from the ferromagnet and suppresses the proximity effect. The ZEP develops in the LDOS only for d-wave pairing and finite barrier strength and its height increases with the increase of the barrier strength.

The ZEP in the LDOS appears also for the d-wave case at the interface of a superconductor with a magnetic DW due to the constructive interference of the ZES that originate from each

domain. For the s-wave case the subgap LDOS is reduced due to the crossed Andreev reflections which transfer Cooper pairs in the superconductor.

In FSF trilayers the pair amplitude is larger in the antiferromagnetic alignment for s-waves. The same is true for d-waves in a higher scale because of an additional pair breaking mechanism due to the pairing symmetry.

Note added in proof. After the paper was accepted we became aware of two interesting works on the proximity effect on d-wave superconductor ferromagnet hybrid structures: the experimental observation of oscillations in the conductance on d-wave superconductor ferromagnet hybrid structures [41] and one theoretical calculation of the proximity effect in d-wave superconductor ferromagnet hybrid structure within quasiclassical theory [42].

References

[1] Sigrist M and Rice T M 1995 *Rev. Mod. Phys.* **67** 503
[2] Van Harlingen D J 1995 *Rev. Mod. Phys.* **67** 515
[3] Tsuei C C and Kirtley J R 2000 *Rev. Mod. Phys.* **72** 969
[4] Kashiwaya S and Tanaka Y 2000 *Rep. Prog. Phys.* **63** 1641
[5] Hilgenkamp H and Mannhart J 2002 *Rev. Mod. Phys.* **74** 485
[6] Kashiwaya S, Tanaka Y, Koyanagi M, Takashima H and Kajimura K 1995 *Phys. Rev.* B **51** 1350
[7] Alff L, Takashima H, Kashiwaya S, Terada N, Ihara H, Tanaka Y, Koyanagi M and Kajimura K 1997 *Phys. Rev.* B **55** 14757
[8] Covington M, Aprili M, Paraoanu E, Greene L H, Xu F, Zhu J and Mirkin C A 1997 *Phys. Rev. Lett.* **79** 277
[9] Wei J Y T, Yeh N-C, Garrigus D F and Strasik M 1998 *Phys. Rev. Lett.* **81** 2542
[10] Iguchi I, Wang W, Yamazaki M, Tanaka Y and Kashiwaya S 2000 *Phys. Rev.* B **62** 6131
[11] Guillou H, Chaussy J, Charalambous M and Pissas M 2002 *Physica* C **382(2–3)** 291
[12] Hu C-R 1994 *Phys. Rev. Lett.* **72** 1526
[13] Tanaka Y and Kashiwaya S 1995 *Phys. Rev. Lett.* **74** 3451
[14] Mélin R 2000 *Europhys. Lett.* **51** 202
[15] Stefanakis N 2001 *Phys. Rev.* B **64** 224502
[16] Zhu J-X, Friedman B and Ting C S 1999 *Phys. Rev.* B **59** 9558
[17] Kashiwaya S, Tanaka Y, Yoshida N and Beasley M R 1999 *Phys. Rev.* B **60** 3572
[18] de Jong M J M and Beenakker C W J 1995 *Phys. Rev. Lett.* **74** 1657
[19] Buzdin A 2001 *Phys. Rev.* B **62** 11377
[20] Baladie I and Buzdin A 2001 *Phys. Rev.* B **64** 224514
[21] Kontos T, Aprili M, Lesueur J and Grison X 2001 *Phys. Rev. Lett.* **86** 304
[22] Bourgeois O, Gandit P, Sulpice A, Chaussy J, Lesueur J and Grison X 2001 *Phys. Rev.* B **63** 064517
[23] Vas'ko V A, Nikolaev K R, Larkin V A, Kraus P A and Goldman A M 1998 *Appl. Phys. Lett.* **73** 844
[24] Fu C-C, Huang Z and Yeh N-C 2002 *Phys. Rev.* B **65** 224516
[25] Tanuma Y, Tanaka Y, Yamashiro M and Kashiwaya S 1998 *Phys. Rev.* B **57** 7997
[26] Martin A M and Annett J F 1998 *Phys. Rev.* B **57** 8709
[27] Zhu J-X, Friedman B and Ting C S 1999 *Phys. Rev.* B **59** 3353
[28] Stefanakis N 2002 *Phys. Rev.* B **66** 024514
[29] Krawiec M, Györffy B L and Annett J F 2002 *Phys. Rev.* B **66** 172505
[30] Krawiec M, Györffy B L and Annett J F 2003 *Physica* C **387** 7
[31] Halterman K and Valls O T 2002 *Phys. Rev.* B **66** 224516
[32] Zhu J-X and Ting C S 2000 *Phys. Rev.* B **61** 1456
[33] Jirari H, Mélin R and Stefanakis N 2003 *Eur. Phys. J.* B **31** 125
[34] Micnas R, Ranninger J and Robaszkiewicz S 1990 *Rev. Mod. Phys.* **62** 113
[35] de Gennes P G 1966 *Superconductivity of Metals and Alloys* (New York: Benjamin)
[36] Soininen P I, Kallin C and Berlinsky A J 1994 *Phys. Rev.* B **50** 13–883
[37] Crétinon L, Favre L, Gupta A, Boisron O, Courtois H, Dupuis V and Pannetier B 2002 *VIIIes Journées de la Matière Condensée (Marseille, 2002)*
[38] Kashiwaya S, Tanaka Y, Koyanagi M and Kajimura K 1996 *Phys. Rev.* B **53** 2667
[39] Giroud M, Hasselbach K, Courtois H, Mailly D and Pannetier B 2003 *Eur. Phys. J.* B **31** 103
[40] Stefanakis N and Mélin R 2002 *Preprint* cond-mat/0209238
[41] Freanat M and Ng K-W 2003 *Preprint* cond-mat/0301081
[42] Faraii Z and Zareyan M 2003 *Preprint* cond-mat/0304336